

1 **Quantification of *nosZ* genes and transcripts in activated sludge microbiomes with novel group-**
2 **specific qPCR methods validated with metagenomic analyses**

3

4 DaeHyun D. Kim^a, Doyoung Park^{a*}, Hyun Yoon^{a†}, Taeho Yun^a, Min Joon Song^a, and Sukhwan
5 Yoon^{a#}

6

7 ^aDepartment of Civil and Environmental Engineering, Korea Advanced Institute of Science and
8 Technology (KAIST)

9

10 **Running Head:** Quantification of *nosZ* with group-specific qPCR

11

12 #Address correspondence to Sukhwan Yoon, syoon80@kaist.ac.kr

13 *Present address: Department of Civil and Environmental Engineering, Georgia Institute of
14 Technology, Atlanta, Georgia, USA

15 †Present address: Department of Civil and Environmental Engineering, Cornell University, Ithaca,
16 New York, USA

17

18

19

20

21

22

23

24

25

26

27

28 **Abstract**

29 Substantial N₂O emission results from activated sludge nitrogen removal processes. The importance of
30 N₂O-reducers possessing NosZ-type N₂O reductases have been recognized as the only N₂O sink *in situ* key
31 to determination of the net N₂O emissions; however, reliable quantification methods for *nosZ* genes and
32 transcripts have yet to be developed. Here, *nosZ* genes and transcripts in activated sludge tank
33 microbiomes were analyzed with the group-specific qPCR assays designed *de novo* combining culture-
34 based and computational approach. A sewage sample was enriched in a batch reactor fed continuous
35 stream of N₂ containing 20-10,000 ppmv N₂O, where 14 genera of potential N₂O-reducers were identified.
36 All available amino acid sequences of NosZ affiliated to these taxa were grouped into five subgroups (two
37 clade I and three clade II groups), and primer/probe sets exclusively and comprehensively targeting the
38 subgroups were designed and validated with *in silico* PCR. Four distinct activated sludge samples from
39 three different wastewater treatment plants in Korea were analyzed with the qPCR assays and the results
40 were validated by comparison with the shotgun metagenome analysis results. With the validated qPCR
41 assays, the *nosZ* genes and transcripts of six additional activated sludge samples were analyzed and the
42 results of the analyses clearly indicated the dominance of two clade II *nosZ* subgroups (*Flavobacterium*-
43 like and *Dechloromonas*-like) among both *nosZ* gene and transcript pools.

44

45 **Introduction**

46 Nitrous oxide (N₂O) is one of the three major greenhouse gases with the largest contributions to
47 global warming, along with CO₂ and CH₄.¹ Although the contribution of N₂O is estimated to be only
48 ~6% of the net greenhouse gas emissions in terms of CO₂eq, which is far less than those of CO₂ and
49 CH₄, eliminating one molecule of N₂O from the atmosphere has the same merit as removing ~300
50 molecule of CO₂ due to its high global warming potential. Besides, N₂O has also been the most
51 consequential ozone depletion agent.^{2,3} Thus, global efforts to curb the increase in atmospheric N₂O
52 concentration are necessitated for sustainable future. A better understanding of the biogeochemical
53 reactions functioning as N₂O sources and sinks in nitrogen-rich anthropogenic environments, e.g.,
54 fertilized agricultural soils and wastewater treatment plants (WWTPs), is especially important for N₂O
55 emission mitigation, as nitrification and denitrification, the biological reactions serving as the major

56 sources of N₂O, occur at consistent a basis in such environments and thus, they have been estimated
57 as the hotspots of N₂O emission to the atmosphere.^{4, 5}

58

59 Particularly, the biological N₂O reduction mediated by Nos-type nitrous oxide reductases (NosZ) has
60 recently attracted immense scientific attention as the sole sink of N₂O on the Earth's surface at non-
61 elevated temperature.⁶⁻⁹ This reaction had been, for long, known merely as one of the stepwise
62 reactions constituting the denitrification pathway.^{4, 10} Only recently has the N₂O-to-N₂ reduction been
63 recognized as an independent energy-conserving reaction, as diverse organisms possessing either
64 conventional clade I and newly-discovered clade II *nosZ* were found to be capable of growth with
65 N₂O as the sole electron acceptor.^{9, 11-13} Several independent research groups have reported difference
66 between clade I and clade II *nosZ*-possessing organisms in terms of their affinities to N₂O, and more
67 specifically, the organisms with *nosZ* closely affiliated to *Dechloromonas* spp. have been reported
68 with particularly low whole-cell Michaelis constants ($K_{m,app}$), suggesting that this group of organisms
69 may be involved in *in situ* consumption of low-concentration N₂O produced via diverse biotic and
70 abiotic processes^{9, 13-16}. The microbial community developed in the laboratory-scale biofilter treating
71 100 ppmv N₂O included the clade II N₂O reducer *Flavobacterium* spp. as the most abundant *nosZ*-
72 carrying organisms, also supporting the significance of clade II N₂O as an important N₂O sink.^{17, 18}

73

74 The NosZ-mediated N₂O reduction has recently been recognized to have an immensely important role
75 in various engineered wastewater treatment systems as the sole sink of N₂O produced from
76 denitrification and nitrification.^{12, 19-23} In these recent studies, attempts have been made to correlate
77 N₂O reduction activities or net N₂O emissions to *nosZ* gene/transcript abundances or the *nosZ*-to-
78 (*nirS+nirK*) abundance ratios. Most, if not all, of these *nosZ* gene quantifications were performed
79 using SYBR Green quantitative polymerase chain reactions (qPCR) targeting the clade I (1840F: 5'-
80 CGCRACGGCAASAAGGTSMSST-3' / 2090R: 5'-CAKRTGCAKSGCRTGGCAGAA-3') and
81 clade II *nosZ* (*nosZ*-II-F: 5'-CTIGGICCIYTKCAYAC-3' / *nosZ*-II-R: 5'-
82 SKSACCTTITRCCITYICG-3').^{24, 25} The reliability of these *nosZ* quantification results were
83 questionable, due to unverified specificity and low amplification efficiency, and even the simplest

84 questions as to whether clade I or clade II *nosZ* were more abundant in nutrient removal bioreactors
85 remains controversial.^{12, 26, 27} In this study, we have developed TaqMan-based qPCR reactions
86 targeting four groups (two clade I *nosZ* groups and two clade II *nosZ* groups) of *nosZ* with
87 amplification efficiency above 90% and verified their coverage and specificity by comparing the
88 quantification data with the results of shotgun metagenome analyses. Anoxic activated sludge samples
89 from anoxic tanks of six conventional wastewater treatment plants in Korea with A2O (anaerobic-
90 anoxic-oxic) configuration were then analyzed with these novel qPCR assays, and without exception,
91 clade II domination of *nosZ* gene and transcript pools was verified.

92

93 **Materials and methods**

94 **Sample collection**

95 The wastewater inoculum for the N₂O enrichment experiments were grab-sampled from the anoxic
96 section of the activated sludge tank at Daejeon municipal WWTP (36°23'5" N 127°24'28" E) in
97 September 2016 (denoted as Daejeon1). Three activated sludge samples for validation of the qPCR
98 assays by comparison with the metagenomics data were collected at the same WWTP (Daejeon2) in
99 February 2019 and two other activated sludge WWTPs located in Gwangju and Gapyeong
100 (35°09'22.4"N 126°49'51.6"E and 37°49'00.1"N 127°31'13.0"E, respectively) in January and
101 February of 2019, respectively. Activated sludge samples from anoxic tanks of six other A2O
102 (anaerobic/anoxic/oxic) WWTPs were then collected for group-specific quantification of *nosZ* genes
103 and transcripts with the developed qPCR assays (Figure S1). Each wastewater sample for analyses of
104 DNA was collected in a 2-L polyethylene bottle filled up to the brim to minimize oxygen ingress. The
105 samples for quantification of *nosZ* transcripts were immediately mixed with the same volume of
106 methanol for RNA fixation.²⁸ The sample bottles were immediately placed in a cooler and
107 transported to the laboratory, where they were stored at -80°C until use.

108

109 **Fed-batch enrichment of activated sludge samples and identification of active N₂O-reducing**
110 **groups**

111 A simple fed-batch bioreactor was constructed for enrichment of active N₂O-reducers in the Daejeon1
112 wastewater sample (Figure S2). A 500-mL glass bottle with a side port (Duran, Mainz, Germany) was
113 fitted with a GL45 cap with three ports. Two of the ports were used as the inlet for N₂O-carrying gas
114 and the gas outlet from the bottle and the remaining port was used for aqueous phase sampling. The
115 side port of the glass bottle was used for sampling of the gaseous phase. The modified MR-1 medium
116 was prepared by adding per 1 L of deionized water, 0.5 g NaCl, 0.41 g sodium acetate, 0.23 g
117 KH₂PO₄, 0.46 g K₂HPO₄, 0.026 g NH₄Cl, 1 ml of 1000X trace metal solution, and 1 mL of 1000X
118 vitamin stock solution.²⁹ The reactor with 200-mL medium (40% of the total reactor volume) was
119 continuously supplied with 0 ppmv, 20 ppmv, 200 ppmv, or 10,000 ppmv N₂O prepared in >99.999%
120 N₂ gas (Samoh Specialty Gas, Daejeon, South Korea) for 30 hours before inoculation. After
121 inoculating the medium with 2 mL of the Daejeon1 sample, the same gas was bubbled through the
122 medium at the volumetric flowrate of 20 mL min⁻¹ to provide the sole electron acceptor N₂O to the
123 microbial culture and maintain the reactor at anoxic condition. The reactor operated with >99.999%
124 N₂ gas served as the control to confirm that the microbial consortia were enriched with N₂O as the
125 electron acceptor and the contribution of O₂ contamination to microbial growth was kept to minimal.
126 The N₂O concentration in the headspace of the reactor was monitored with a HP6890 Series gas
127 chromatography fitted with an HP-PLOT/Q column and an electron capture detector (Agilent, Palo
128 Alto, CA), with the injector, oven and detector temperatures set to 200, 85, and 250 °C, respectively.³⁰
129 The O₂ concentration in the fed-batch reactor was monitored with a FireSting-O₂ oxygen meter
130 (Pyroscience, Aachen, Germany); however, due to the relatively high detection limit of the sensor (the
131 gas phase concentration of ~0.1% v/v), complete absence of O₂ was not guaranteed.
132
133 The growth of bacterial population in the reactor was monitored with qPCR using TaqMan chemistry
134 targeting the conserved region of eubacterial 16S rRNA genes. At each sampling time point, an 1.5-
135 mL aliquot was collected from the aqueous phase of the reactor and DNA was extracted from the
136 pellets using DNeasy Blood & Tissue Kit (Qiagen, Hilden, Germany) following the protocol provided
137 by the manufacturer. Quantitative PCR was performed with the 1055f (5'-ATGGCTGTCGTCAGCT-
138 3') / 1392r (5'-ACGGGCGGTGTGTAC-3') / Bac1115Probe (5'-CAACGAGCGCAACCC-3')

139 primer and probe set targeting a conserved region of bacterial 16S rRNA genes using a QuantStudio3
140 platform (Thermo Fisher Scientific, Waltham, MA).³¹ Incubation was halted when the population of
141 the enrichment reached a plateau, as indicated by three consecutive measurements without increased
142 gene counts. The reactor was dismantled and the aqueous phase was collected for microbial
143 composition analysis. The hypervariable V6–8 region of the 16S rRNA gene was amplified with 926F:
144 5'-AAACTYAAAKGAATTGRCGG-3' / 1392R: 5'-ACGGGCGGTGTGTRC-3' primer set and
145 MiSeq sequencing of the amplicons was outsourced to Macrogen Inc. (Seoul, Korea). The raw
146 sequence reads were deposited in the NCBI short reads archive (SRA) database (accession:
147 PRJNA552413) and were processed using the QIIME pipeline v 1.9.1 (detailed computational method
148 provided in the supplementary information).

149

150 **Design of degenerate primers and probes for group-specific qPCR of *nosZ* genes**

151 The genera assigned to the OTUs with the relative abundances higher than 0.3% in any of the reactor
152 microbial communities were selected. All *nosZ* gene sequences and corresponding translated NosZ
153 amino acid sequences belonging to the organisms affiliated to these genera were extracted from the
154 Uniprot (www.uniprot.org) database (accessed in March 2017) (Table S1). The curated pools of
155 *nosZ*/NosZ sequence data included, in total, 174 nucleotide sequences and the corresponding amino
156 acid sequences from 14 distinct genera. Subsequently, a multiple sequence alignment was performed
157 with these amino acid sequences, using MUSCLE algorithm with the parameters set to the default
158 values.³² The NosZ phylogenetic tree was constructed using the neighbor-joining method in MEGA
159 7.0 with the bootstrap value set to 500.³³ The *nosZ* gene sequences were clustered into five groups
160 (NosZG1-5) according to the positions of the corresponding NosZ sequences in the phylogenetic tree,
161 which consisted of five phylogenetically distinct subbranches.

162

163 For each *nosZ* group, a primers and probe set was designed using the PriMux software to
164 comprehensively and exclusively target the *nosZ* gene sequences within the group.³⁴ The parameters
165 were modified from the default values to obtain the optimal candidate degenerate oligonucleotide
166 sequences for qPCR (length: 18-24 bp, amplicon size: 80-400 bp, T_m: 56-62°C for primers and 68 -

167 72°C for probes). Several candidate primers and probe sets were generated for each *nosZ* group,
168 implementing the *min*, *max*, and *combo* algorithms of the Primux software. The performance of each
169 candidate primers and probe set was predicted with *in silico* PCR performed with the simulate_PCR
170 software against all complete genome sequences of the organisms belonging to each of the five *nosZ*
171 groups (Table S1).^{34, 35} Coverage within the target *nosZ* group and mutual exclusivity across the
172 groups were the two major criteria for assessment of the candidate primers and probe sets. The *in*
173 *silico* PCR tests were also performed against the complete genomes of 50 bacterial strains lacking
174 *nosZ* to preclude the possibility of unspecific amplification.

175

176 **Construction of calibration curves for the designed primer and probe sets using model N₂O** 177 **reducer strains**

178 A model organism from each group of the selected *nosZ* gene(s) was used for construction of the
179 calibration curve. The selected model organisms were *Pseudomonas stutzeri* DCP-Ps1 (NosZG1),
180 *Acidovorax soli* DSM25157 (NosZG2), *Flavobacterium aquatile* LMG4008 (NosZG3),
181 *Ignavibacterium album* JCM16511 (NosZG4), and *Dechloromonas aromatica* RCB (NosZG5).
182 *Acidovorax soli* DSM25157 and *F. aquatile* LMG4008 were acquired from Korean Collection for
183 Type Cultures and *I. album* JCM16511 from Japanese Collection of Microorganisms. The axenic
184 batch cultures of these organisms were prepared as previously described in the literature or using the
185 media and incubation conditions specified by the distributors. The cells were harvested at OD_{600nm} =
186 0.1 and the *nosZ* gene(s) in the DNA extracted from the cell pellets were amplified using the designed
187 primers. The calibration curve for each qPCR reaction was constructed using ten-fold serial dilutions
188 of PCR[®] 2.1 vectors (Invitrogen, Carlsbad, CA) carrying the *nosZ* amplicons. A uniform thermocycle
189 was used for the qPCR: 95°C for 10 min and 40 cycles of 95 °C for 30 s, 58 °C for 60 s, and 72 °C for
190 60 s.

191

192 **Group specific quantitative PCR targeting *nosZ* gene and transcripts in activated sludge** 193 **samples**

194 The group-specific quantification of the *nosZ* genes and transcripts in the activated sludge samples
195 were performed with the designed primer and probe sets (Table 1) on a QuantStudio 3 real-time PCR
196 instrument using TaqMan detection chemistry (FAM as the reporter and NFQ-MGB as the quencher).
197 DNeasy Blood & Tissue Kit (QIAGEN) was used to extract DNA from the activated sludge samples.
198 From the methanol-treated samples, RNA was extracted with RNeasy Mini Kit (Qiagen), purified
199 with DNase I (Qiagen) and RNeasy MinElute Cleanup Kit (Qiagen), and reverse-transcribed with
200 Superscript[®] III (Thermo Fisher Scientific), as described previously.³⁶ The luciferase control mRNA
201 (Promega, Madison, WI, USA) was added as the internal standard to account for RNA loss during the
202 process. Each 20- μ L qPCR reaction mix contained 10 μ L of 2X TaqMan master mix (Applied
203 Biosystems, Foster city, CA, USA), 5 μ M each of the forward and reverse primers, 0.5 μ M of the
204 probe, and 2 μ L of the DNA or cDNA. Calibration curves prepared with dilution series of the PCR
205 amplicons were used to calculate the copy numbers of the targeted genes from the C_t values.
206 Eubacterial 16S rRNA genes in the extracted DNA samples were quantified using the
207 1055F/1392R/Bac115Probe set for quantification of total bacterial population in the activated sludge
208 samples (Table S2). The copy numbers of the targeted *nosZ* genes in the wastewater samples were
209 normalized with the 16S rRNA gene copy numbers to facilitate comparison with the relative
210 abundances of the *nosZ* groups from the metagenomic analyses.

211

212 The PCR amplicons of the Daejeon1 sample amplified with NosZG1-5 primer sets were sequenced
213 using Illumina Miseq platform (San Diego, CA) at the Center for Health Genomics and Informatics at
214 University of Calgary. The raw sequence reads have been deposited in the SRA database (accession
215 number: PRJNA552418). After quality trimming and merging of the paired-end sequences, the
216 sequences without the probe-binding region were removed, and the remaining reads were clustered
217 into OTUs with 0.97 cut-off using cd-hit-est v. 4.6.³⁷ The OTUs were annotated using blastx against
218 the bacterial Refseq database downloaded in June, 2018, with the e value cut off set to 10^{-3} and word
219 size to 3 and no seg option selected,

220

221 **Computational quantification of *nosZ* genes from shotgun metagenomes of the activated sludge**
222 **samples**

223 The DNA samples for shotgun metagenome sequencing were extracted with DNeasy PowerSoil Kit
224 (Qiagen) from 50 mL each of the four activated sludge samples collected for validation of the qPCR
225 assays. Sequencing of the metagenomic DNA was performed at Macrogen Inc., where HiSeq X Ten
226 sequencing platform (Illumina, San Diego, CA) was used for generating 5-10 Gb of paired-end reads
227 data with 150-bp read length. The raw sequence reads have been deposited in the NCBI short reads
228 archive (SRA) database (accession numbers: PRJNA552406).

229

230 The raw reads were then processed using Trimmomatic v0.36 software with the parameters set to the
231 default values.³⁸ The trimmed reads were translated *in silico* into amino acid sequences using all six
232 possible reading frames and screened for clade I and II *nosZ* sequences using hidden Markov models
233 (HMM). The two HMM algorithms for clade II *nosZ* were downloaded from the Fungene database
234 (accessed in October 2016). As the HMM for clade I *nosZ* in the database had specificity issues, the
235 HMM algorithm was constructed *de novo* using *hmmbuild* command of HMMER v3.1b1. The clade I
236 *NosZ* sequences used to build the HMM were manually curated from the pool of *NosZ* sequences
237 downloaded from the NCBI database (accessed in October 2016), to represent diverse subgroups
238 within the clade (Table S3).^{8, 11} The candidate partial *NosZ* sequences were extracted from the
239 translated shotgun metagenome reads using the *hmmsearch* command of HMMER v3.1b1 with the e
240 value cutoff set to 10^{-5} . The nucleotide sequence reads corresponding to the extracted partial *NosZ*
241 sequences (in separate bins for clade I and clade II *NosZ*) were assembled into contigs using
242 metaSPAdes v3.12.0 with parameters set to default values.³⁹ The assembled contigs with lengths
243 shorter than 200 bp were filtered out. The overlapping contigs appearing in both clade I and clade II
244 *NosZ* bins were identified by clustering the two sets of contigs against each other with a nucleotide
245 identity cutoff of 1.0. These overlapping contigs were manually called to the correct bin according to
246 the BLASTX results. The trimmed sequence reads were then mapped onto the contigs in the *nosZ*
247 bins using Bowtie2 v2.2.6, yielding sequence alignments for the contigs and the mapped reads. The
248 alignment files were further processed using samtools v0.1.19, and the PCR duplicates were removed

249 using MarkDuplicates function of picard-tools v1.105.⁴⁰ The sequence coverages of the contigs were
250 calculated using bedtools v2.17.0. The number of reads mapped on to the contigs were normalized
251 with the lengths of the respective contigs. The contigs were assigned taxonomic classification using
252 blastx, and distributed to the NosZG1-5 bins based on their taxonomic affiliations (Table S4). The
253 contigs without matching sequence were binned as ‘other *nosZ* sequences’. The attempt to use 16S
254 rRNA sequences extracted with Meta-RNA and assembled with EMIRGE as the template for
255 mapping was not successful, as the coverage of the extracted 16S rRNA sequences turned out to be an
256 order of magnitude lower than the *rpoB* coverage (Data not shown).^{41,42} Thus, the sequence coverage
257 of *rpoB* gene, a single-copy housekeeping gene, was used for normalization of the *nosZ* abundance
258 data. The HMM algorithm for *rpoB* was downloaded from the Fungene database.

259

260 **Results**

261 **Active N₂O reducers enriched in fed-batch incubation with varying N₂O concentrations**

262 The microbial communities of the three N₂O-reducing enrichments, each prepared with different N₂O
263 concentrations, were analyzed to identify active N₂O-reducing groups of microorganisms (Table S5).
264 Screening for operational taxonomic units (OTUs) with >0.3% abundance in any of the three
265 enrichments yielded 69 OTUs assigned to 33 genera in total, and 14 of these genera were identified
266 with phylogenetic subgroups harboring clade I or clade II *nosZ*. The OTUs belonging to these
267 putatively *nosZ*-harboring genera amounted to 50.8% – 63.2% of the total microbial population in the
268 enrichments. The abundances of the genera putatively harboring clade II *nosZ* were observed to be
269 greater than those of the genera harboring clade I of *nosZ* (Table S5). In the enrichment incubated
270 with 20 ppmv N₂O, *Cloacibacterium* (18.9%), *Flavobacterium* (14.2%), and *Acidovorax* (13.5%)
271 were identified as the dominant genera. *Dechloromonas* (17.3%) and *Flavobacterium* (15.8%) were
272 the dominant genera in the 200 ppmv enrichment, and *Dechloromonas* was the predominant
273 population in the enrichment incubated with 10,000 ppmv of N₂O, constituting 46.0% of the total
274 microbial population.

275

276 **Designing of the degenerate *nosZ* primer/probe sets**

277 With the 174 translated NosZ sequences affiliated to the 14 genera putatively harboring active N₂O-
278 reducing organisms identified in the activated sludge enrichments, a phylogenetic tree composed of
279 five distinct branches (NosZG1 – NosZG5) was constructed (Figure S3). NosZG1 and NosZG2 were
280 identified as clade I NosZ and NosZG3-NosZG5 as clade II NosZ. After the iterative process of
281 designing candidate primers and probe sets and performing *in silico* PCR tests, the final sets of
282 degenerate primers/probe sets were designed to comprehensively and exclusively target the five *nosZ*
283 groups (Table 1). The *in-silico* PCR performed against 174 genomes from which the target *nosZ*
284 sequences were extracted and 50 genomes without *nosZ* confirmed the high levels of coverage (57.3-
285 100%) and complete exclusivity for all five degenerate primers/probe sets (Table 1). The qPCR
286 calibration curves were constructed with the selected model organisms (Figure S4, Table S6), and
287 despite the high levels of degeneracy (up to 110592), amplification efficiencies above 90% were
288 attained for all five primer and probe sets after rigorous optimization process.

289

290 **Cross-checking of the group-specific qPCR quantification of *nosZ* genes with shotgun** 291 **metagenome analyses**

292 The *nosZ* gene abundances in four distinct activated sludge samples were quantified using the newly
293 designed qPCR assays, and the *nosZ* sequences extracted from the shotgun metagenomes of these
294 same samples were quantitatively analyzed in parallel, for cross-checking of the qPCR results (Figure
295 1). The qPCR results of the four activated sludge samples invariably showed the dominance of the
296 clade II *nosZ* genes (NosZG3 and NosZG5) over clade I *nosZ* genes (NosZG1 and NosZG2), with at
297 least five-fold higher copy numbers (Figure 2). The qPCR targeting the NosZG4 group failed to
298 amplify the clade II *nosZ* belonging to this group. The NosZG4 primers/probe set was designed from
299 a single complete genome (*Ignavibacterium album*) and six sequences from metagenome assembled
300 genomes (MAGs), which may have been insufficient to cover the sequence divergence of this *nosZ*
301 subgroup.

302

303 The distribution of the *nosZ* sequences extracted from the shotgun metagenomes (Table S7) were also
304 severely biased towards clade II. The compositions of the *nosZ* genes exhibited high level of

305 similarity across the activated sludge samples. The calculated relative abundances of the two most
306 abundant groups, NosZG3 and NosZG5, were relatively consistent across the samples, varying by less
307 than 1.7-fold. The contributions of NosZG1 and NosZG2 to the total *nosZ* gene abundances were
308 minor in all of the samples and largely variable. The fold differences between the samples with the
309 highest relative abundance of NosZG1 and NosZG2 and those with the lowest abundance were 3.5
310 and 2.3, respectively. The *nosZ* genes sorted as NosZG4 constituted <1.2% of the total *nosZ* genes
311 grouped as NosZG1-NosZG5, suggesting that this *nosZ* group has less significant role in N₂O
312 reduction in activated sludge tanks than other analyzed groups.

313

314 As the qPCR data were normalized with the eubacterial 16S rRNA copy numbers and the
315 metagenome-derived relative abundance data were normalized with the sequence coverages of the
316 single-copy housekeeping gene *rpoB*, direct comparison of the outcomes was not possible.
317 Theoretically, however, the ratios of the *nosZ/rpoB* (metagenome) to *nosZ/16S* (qPCR) could be used
318 as indicators of reliability of the qPCR assays, with consistency in the ratios across the *nosZ* groups
319 indicating high reliability. The *nosZ/rpoB*-to-*nosZ/16S* ratios were within a narrow range between 1.6
320 and 2.4 for NosZG5 across the four activated sludge samples. For an unidentified reason, broad gaps
321 between the NosZG1-3 qPCR and the metagenomics data were observed with the Daejeon1 sample.
322 Excluding these results, the *nosZ/rpoB*-to-*nosZ/16S* ratio varied from 3.3 to 7.2 for NosZG3, and the
323 *nosZ/rpoB*-to-*nosZ/16S* ratios of NosZG1 and NosZG2 ranged from 1.9 to 2.1 and from 1.9 to 9.2,
324 respectively. The *nosZ/16S*-to-*nosZ/rpoB* ratios of 12 out of the 16 qPCR assays performed
325 (excluding NosZG4) were within the range between 1.5 and 9.2, indicating that the group-specific
326 qPCR assays enabled reliable quantification of *nosZ* genes.

327

328 The *nosZ* amplicons of the Daejeon1 sample, amplified with the newly-designed qPCR primers, were
329 sequenced and analyzed to check whether the qPCR reactions were comprehensive and mutually
330 exclusive (Figure 3). As the NosZG4 primers failed to amplify the targeted genes, NosZG4 was
331 excluded from the downstream analysis. The *nosZ* genes of putative active N₂O reducers captured by
332 the NosZG1 and NosZG2 primer sets accounted for 54.2% of the entire pool of the clade I *nosZ* genes

333 extracted from the shotgun metagenome. The NosZG3 and NosZG5 primer sets captured 63.4% of the
334 clade II *nosZ* genes recovered from the metagenome (Figure S5). No amplification outside the
335 targeted group occurred for any of the primers, confirming the complete mutual exclusivity of these
336 primers. Each of the qPCR assays were comprehensive within its target groups, as analyzed *nosZ*
337 amplicon sequences covered all genera originally targeted by each primer and probe set.

338

339 Overall, the OTUs identified to be abundant from sequence analyses of the PCR amplicons coincided
340 with the dominant *nosZ* OTUs from shotgun metagenome analysis. The OTUs affiliated to
341 *Rhodobacter capsulatus*, Rhodobacteraceae bacterium QY30, *Hyphomicrobium denitrificans*, and
342 *Bradyrhizobium* sp. were the dominant OTUs among the OTUs NosZG1 amplicons. The two most
343 abundant *nosZ* OTUs among the NosZG3 amplicons were affiliated to *Flavobacterium columnare* and
344 *Niastella koreensis*, which were also the most abundant *nosZ* taxa according to the metagenome
345 analyses. Discrepancies between the amplicon sequencing data and the shotgun metagenome data
346 were observed for NosZG2 and NosZG5 to some degree. The OTUs assigned to the genus *Thauera*
347 and *Ruvrivorax gelatinosus* were the dominant among NosZG2, constituting 50.4% of the amplicons,
348 but together constituted only 2.2% of the metagenome-derived *nosZ* sequences belonging to this
349 group. Instead, an OTU affiliated to *Ramlibacter tataouinensis*, closely related to *R. gelatinosus*, was
350 recovered in high relative abundance (15.4%) in the metagenome-derived *nosZ* pool. Likewise, the
351 low relative abundance of the OTUs affiliated to *Dechloromonas aromatica* (0.2%) in the NosZG5
352 amplicons was coupled to the high relative abundance of the *nosZ* OTU affiliated to the *Azospira*
353 *oryzae* (54.6%) with >96% translated amino acid identity within the amplified region. Thus, the
354 observed discrepancy may be due to ambiguous OTU assignment among the closely related taxa.

355

356 The TaqMan-based qPCR assays were also compared with the most frequently used qPCR assays for
357 clade I and clade II *nosZ* using SYBR green detection chemistry (Figure S6). Despite the low
358 amplification efficiency (79.3%), the abundances of clade I *nosZ*, as determined with the SYBR
359 Green assays, were relatively consistent with the cumulative abundances of NosZG1 and NosZG2
360 determined with the TaqMan qPCR assays, except for Daejeon1 sample, where the SYBR Green

361 qPCR yielded 87 times lower copy numbers than the TaqMan qPCR. The SYBR Green qPCR with
362 nosZII-F–nosZII-R primer set, with a subpar amplification efficiency of 61.9%, underestimated the
363 clade II *nosZ* copy numbers by several orders of magnitudes for three of the four analyzed samples,
364 with the largest difference (1.8×10^3 -fold) observed with the Daejeon1 sample. The importance of the
365 clade II *nosZ* among the N₂O-reducing microbial community in these activated sludge samples would
366 have gone unnoticed due to this underestimation, if the conventional qPCR assays were used as the
367 sole means of *nosZ* quantification.

368

369 **Quantitative analyses of *nosZ* genes and transcripts in activated sludge microbiomes**

370 With the new group-specific *nosZ* primers, the activated sludge microbiomes from anoxic tanks of six
371 A2O WWTPs apart from those used for development and cross-checking processes were analyzed for
372 the *nosZ* gene and transcript abundances (Figure 4). As observed with the samples from Daejeon1,
373 Daejeon2, Gwangju, and Gapyeong, the clade II *nosZ* (amplified with NosZG3 and NosZG5), were at
374 least three-fold more abundant than the clade I *nosZ* (amplified with NosZG1 and NosZG2) in terms
375 of gene abundance. The *Dechloromonas*-like *nosZ* genes (NosZG5) was the most abundant *nosZ*
376 group in all samples but from Busan WWTP, where the abundance of *Flavobacterium*-like *nosZ*
377 genes (NosZG3) was statistically similar to this group. The transcript profiles further highlighted the
378 significance of clade II *nosZ* in activated sludge microbiomes. Due to the lower gene abundance and
379 generally low level of transcription observed for clade I *nosZ* (transcript-to-gene ratios of <1.0 for
380 both NosZG1 and NosZG2 in five out of six samples), transcription of the clade I *nosZ* was at least an
381 order of magnitude lower than that of the clade II *nosZ* in all samples. The *Pseudomonas*-like *nosZ*
382 (NosZG1) had remarkably low transcription level (transcript-to-gene ratios of <0.01) in all samples
383 but from Busan WWTP, suggesting irrelevance of this *nosZ* group as an N₂O sink in the activated
384 sludge tanks. The relative importance of NosZG3 and NosZG5 is difficult to fathom, as *nosZ*
385 transcripts targeted by NosZG3 were significantly more abundant in the sample from Busan WWTP
386 ($p < 0.05$), while NosZG5 was significantly more abundant in the samples from three other WWTPs
387 ($p < 0.05$).

388

389 **Discussion**

390 Quantification of the functional genes encoding the nitrogen cycle enzymes (e.g., bacterial/archaeal
391 *amoA*, comammox *amoA*, *nrfA*, and clade I and II *nosZ*) has been used in increasing number of
392 studies across diverse disciplines of environmental sciences and engineering, as predictors of nitrogen
393 cycling activity in diverse soil and aquatic environments.⁴³⁻⁴⁶ Despite the frequent use of qPCR in
394 determining the potential N₂O-reducing populations, i.e., clade I and clade II *nosZ*-possessing
395 microorganisms, the predictability of qPCR quantification has rarely been scrutinized in the previous
396 studies. The new group-specific qPCR assays exhibited definite advantages over these frequently used
397 primers. Although the targets were limited to the groups of *nosZ*-possessing organisms enriched with
398 N₂O in *ex situ* cultures, the copy numbers obtained were, in many cases, orders of magnitudes larger
399 than those measured using previous primer sets. The diversity of the sequences recovered in the
400 amplicon sequence indicates the exhaustive coverages of the qPCR assays developed in this study
401 within the targeted groups. Most of the major *nosZ* OTUs (>1% in relative abundance) recovered in
402 metagenome-based *nosZ* profiling of the examined activated sludge samples were amplified with
403 exactly one of the four primer sets, thus confirming the absolute mutual exclusiveness of the
404 primers/probe sets. Any methods for quantification of functional genes are prone to error, and the
405 *nosZ* qPCR methods developed here also have certain deficiencies, including inability to amplify *nosZ*
406 genes affiliated to relatively abundant *Iganvibacterium* spp. In designing the group-specific primers, a
407 trade-off between coverage and mutual exclusivity was inevitable, which could have been the cause
408 of modest discrepancy with the metagenome data. Nevertheless, despite these drawbacks, there is
409 little doubt that the qPCR assays developed in this study are the most reliable tools for real-time
410 quantification of the environmentally significant *nosZ* genes available to date.

411

412 The clade II *nosZ*-possessing organisms of the *Flavobacterium* (amplified with NosZG3),
413 *Dechloromonas*, and *Azospira* (amplified with NosZG5) genera have previously been characterized
414 with high-affinity reduction of N₂O.^{13, 14} The whole-cell half-saturation constants as low as 0.324 μM
415 has been reported for these groups of N₂O reducers. The *nosZ* gene and transcript pools of all six of
416 the activated sludge samples were dominated by these clade II *nosZ* (targeted by NosZG3 and

417 NosZG5). This observation, along with the high transcript-to-gene ratios support the previous
418 hypothesis that the clade II *nosZ*, with higher affinity to N₂O, may have consequential role in reducing
419 N₂O emissions from soil and aquatic environments, including the activated sludge tanks.^{15, 47} The low
420 transcript-to-gene ratios of the clade I *nosZ* (<0.1 in five out of six samples) targeted by NosZG1 and
421 NosZG2 were also notable in the *nosZ* transcript profiles. The organisms possessing clade I *nosZ*
422 genes, being almost exclusively denitrifiers, may favor upstream steps of denitrification reaction in
423 the anoxic activated sludge tanks, where NO₃⁻ and/or NO₂⁻ are constantly available at millimolar
424 concentrations and N₂O is immediately consumed by their high-affinity cohabitants, which may
425 prefer N₂O to NO₃⁻ or NO₂⁻. More physiological evidences are warranted in the future research,
426 however, to verify whether such hypothetical ‘division of labor’ really exists, as any further
427 extrapolation from the *nosZ* transcription data alone would be an over-interpretation.

428

429 The major *nosZ*-possessing organisms identified in the qPCR and metagenomic analyses differ greatly
430 from the major *nosZ*-possessing populations of the agricultural soils analyzed previously with shotgun
431 metagenome sequencing.⁴⁸ None of the six most abundant *nosZ* phylogenetic groups in the Havana
432 and Urbana agricultural research site soils (the *nosZ* genes affiliated to *Anaeromyxobacter*, *Opitutus*,
433 *Hydrogenobacter*, *Ignavibacterium*, *Dyedobacter*, and *Gemmatimonas*) was identified as a major
434 population in any of the activated sludge samples examined in this study. Neither were they enriched
435 with N₂O to high relative abundance (e.g., >1%) in the fed-batch reactor. Of the organisms affiliated
436 to these genera, *Anaeromyxobacter dehalogenans* and *Gemmatimonas aurentiaca* have been
437 confirmed of N₂O reduction activity; however, the N₂O reduction rates measured *in vitro* were orders
438 of magnitudes lower for these organisms than other examined N₂O-reducing organisms throughout
439 the entire range of N₂O concentration, and *G. aurantiaca* lacked the capability to utilize N₂O as the
440 growth substrate.^{11, 13, 30} The differences in the compositions of the *nosZ*-possessing populations may
441 be attributed to the inherent difference in the rates of the biochemical turnover processes in WWTP
442 activated sludges and soils. Rapid nitrogen cycling reactions take place on a constant basis in WWTPs,
443 while the time scale of the biogeochemical processes in agricultural soils is orders of magnitude
444 longer and often, nitrogen supply provided through fertilization and plant exudation is sparse and

445 sporadic.⁴⁹ Besides, upland agricultural soils are often well-aerated and thus, the capability of N₂O
446 utilization would not provide specific benefits to the *nosZ*-harboring organisms at ordinary dry
447 conditions.⁵⁰ In fact, incubation of soil microbial consortium with N₂O in the same fed-batch
448 cultivation resulted in enrichment of the same organismal groups as those observed in the activated
449 sludge enrichments (e.g., *Pseudomonas*, *Flavobacterium*, *Acidovorax*, and *Chryseobacterium*),
450 suggesting that under occasions of pulse stimulation of denitrification and N₂O reduction, e.g.,
451 flooding events immediately following fertilization, these organisms may become the relevant N₂O
452 sinks in soils, as well (Table S8). Besides, none of the 14 *nosZ*-carrying genera enriched with N₂O in
453 this study from either the activated sludge and soil belonged to the taxa identified as non-denitrifying
454 N₂O reducers suggesting that the abundance of non-denitrifier taxa, *per se*, may not be a measure of
455 the N₂O sink capability, as previously proposed.

456

457 **Acknowledgements**

458 This work was financially supported by “the R&D Center for reduction of Non-CO₂ Greenhouse
459 Gases (Grant No. 2017002420002)” funded by Korea Ministry of Environment (MOE).

460

461 **Reference**

462 (1) Ciais, P.; Sabine, C.; Bala, G.; Bopp, L.; Brovkin, V.; Canadell, J.; Chhabra, A.;
463 DeFries, R.; Galloway, J.; Heimann, M.; Jones, C.; Le Quere, C.; Myneni, R. B.; Piao,
464 S.; Thornton, P., Carbon and other biogeochemical cycles. In *Climate change 2013:
465 The physical science basis. Contribution of working group I to the fifth assessment
466 report of the Intergovernmental Panel on Climate Change*, Stocker, T. F.; Qin, D.;
467 Plattner, G.-K.; Tignor, M.; Allen, S. K.; Boschung, J.; Nauels, A.; Xia, Y.; Bex, V.;
468 Midgley, P. M., Eds. Cambridge University Press: Cambridge, United Kingdom, New
469 York, NY, USA, 2013; pp 465-570. [http://www.ipcc.ch/pdf/assessment-
470 report/ar5/wg1/WG1AR5_Chapter06_FINAL.pdf](http://www.ipcc.ch/pdf/assessment-report/ar5/wg1/WG1AR5_Chapter06_FINAL.pdf)

- 471 (2) Ravishankara, A. R.; Daniel, J. S.; Portmann, R. W. Nitrous oxide (N₂O): the dominant
472 ozone-depleting substance emitted in the 21st century. *Science* **2009**, *326*, (5949), 123-
473 125.
- 474 (3) Portmann, R. W.; Daniel, J. S.; Ravishankara, A. R. Stratospheric ozone depletion due
475 to nitrous oxide: influences of other gases. *Phil. Trans. R. Soc. B* **2012**, *367*, (1593),
476 1256-1264.
- 477 (4) Yoon, S.; Song, B.; Phillips, R. L.; Chang, J.; Song, M. J. Ecological and physiological
478 implications of nitrogen oxide reduction pathways on greenhouse gas emissions in
479 agroecosystems. *FEMS Microbiol. Ecol.* **2019**, *95*, (6), fiz066.
- 480 (5) Law, Y.; Ye, L.; Pan, Y.; Yuan, Z. Nitrous oxide emissions from wastewater treatment
481 processes. *Phil. Trans. R. Soc. B* **2012**, *367*, (1593), 1265-1277.
- 482 (6) Thomson, A. J.; Giannopoulos, G.; Pretty, J.; Baggs, E. M.; Richardson, D. J. *Philos*
483 *Trans Royal Soc B* **2012**, *367*, (1593), 1157-1168.
- 484 (7) Frutos, O. D.; Quijano, G.; Aizpuru, A.; Muñoz, R. A state-of-the-art review on nitrous
485 oxide control from waste treatment and industrial sources. *Biotechnol. Adv.* **2018**, *36*,
486 (4), 1025-1037.
- 487 (8) Hallin, S.; Philippot, L.; Löffler, F. E.; Sanford, R. A.; Jones, C. M. Genomics and
488 ecology of novel N₂O-reducing microorganisms. *Trends Microbiol.* **2017**, *26*, (1), 43-
489 55.
- 490 (9) Suenaga, T.; Hori, T.; Riya, S.; Hosomi, M.; Smets, B. F.; Terada, A. Enrichment,
491 isolation, and characterization of high-affinity N₂O-reducing bacteria in a gas-
492 permeable membrane reactor. *Environ. Sci. Technol.* **2019**, *in press*; DOI:
493 10.1021/acs.est.9b02237
- 494 (10) Zumft, W. G. Cell biology and molecular basis of denitrification. *Microbiol. Mol. Biol.*
495 *Rev.* **1997**, *61*, (4), 533-616.

- 496 (11) Sanford, R. A.; Wagner, D. D.; Wu, Q.; Chee-Sanford, J. C.; Thomas, S. H.; Cruz-
497 García, C.; Rodríguez, G.; Massol-Deyá; Krishnani, K. K.; Ritalahti, K. M.; Nissen, S.;
498 Konstantinidis, K. T.; Löffler, F. E. Unexpected nondenitrifier nitrous oxide reductase
499 gene diversity and abundance in soils. *Proc. Natl Acad Sci* **2012**, *109*, (48), 19709-
500 19714.
- 501 (12) Conthe, M.; Wittorf, L.; Kuenen, J. G.; Kleerebezem, R.; van Loosdrecht, M. C. M.;
502 Hallin, S. Life on N₂O: deciphering the ecophysiology of N₂O respiring bacterial
503 communities in a continuous culture. *ISME J.* **2018**, *12*, (4), 1142-1153.
- 504 (13) Yoon, S.; Nissen, S.; Park, D.; Sanford, R. A.; Löffler, F. E. Nitrous oxide reduction
505 kinetics distinguish bacteria harboring clade I versus clade II NosZ. *Appl. Environ.*
506 *Microbiol.* **2016**, *82*, (13),3793-3800.
- 507 (14) Suenaga, T.; Riya, S.; Hosomi, M.; Terada, A. Biokinetic characterization and activities
508 of N₂O-reducing bacteria in response to various oxygen levels. *Front. Microbiol.* **2018**,
509 *9*, 697.
- 510 (15) Jones, C. M.; Spor, A.; Brennan, F. P.; Breuil, M.-C.; Bru, D.; Lemanceau, P.; Griffiths,
511 B.; Hallin, S.; Philippot, L. Recently identified microbial guild mediates soil N₂O sink
512 capacity. *Nat. Clim. Change* **2014**, *4*, 801-805.
- 513 (16) Domeignoz-Horta, L. A.; Spor, A.; Bru, D.; Breuil, M.-C.; Bizouard, F.; Leonard, J.;
514 Philippot, L. The diversity of the N₂O reducers matters for the N₂O:N₂ denitrification
515 end-product ratio across an annual and a perennial cropping system. *Front. Microbiol.*
516 **2015**, *6*, 971
- 517 (17) Yoon, H.; Song, M. J.; Yoon, S. Design and feasibility analysis of a self-sustaining
518 biofiltration system for removal of low concentration N₂O emitted from wastewater
519 treatment plants. *Environ. Sci. Technol.* **2017**, *51*, (18), 10736-10745.

- 520 (18) Yoon, H.; Song, M. J.; Kim, D. D.; Sabba, F.; Yoon, S. A serial biofiltration system for
521 effective removal of low-concentration nitrous oxide in oxic gas streams: mathematical
522 modeling of reactor performance and experimental validation. *Environ. Sci. Technol.*
523 **2019**, *53*, (4), 2063-2074.
- 524 (19) Paranychianakis, N. V.; Tsiknia, M.; Kalogerakis, N. Pathways regulating the removal
525 of nitrogen in planted and unplanted subsurface flow constructed wetlands. *Water Res.*
526 **2016**, *102*, 321-329.
- 527 (20) Conthe, M.; Kuenen, J. G.; Kleerebezem, R.; van Loosdrecht, M. C. M. Exploring
528 microbial N₂O reduction: a continuous enrichment in nitrogen free medium. *Environ.*
529 *Microbiol. Rep.* **2018**, *10*, (1), 102-107.
- 530 (21) Boonnorat, J.; Techkarnjanaruk, S.; Honda, R.; Ghimire, A.; Angthong, S.; Rojviroon,
531 T.; Phanwilai, S. Enhanced micropollutant biodegradation and assessment of nitrous
532 oxide concentration reduction in wastewater treated by acclimatized sludge
533 bioaugmentation. *Sci. Tot. Environ.* **2018**, *637*, 771-779.
- 534 (22) Song, K.; Suenaga, T.; Harper, W. F.; Hori, T.; Riya, S.; Hosomi, M.; Terada, A.
535 Effects of aeration and internal recycle flow on nitrous oxide emissions from a
536 modified Ludzak–Ettinger process fed with glycerol. *Environ. Sci. Pollut. Res.* **2015**,
537 *22*, (24), 19562-19570.
- 538 (23) Vieira, A.; Galinha, C. F.; Oehmen, A.; Carvalho, G. The link between nitrous oxide
539 emissions, microbial community profile and function from three full-scale WWTPs. *Sci.*
540 *Tot. Environ.* **2019**, *651*, 2460-2472.
- 541 (24) Henry, S.; Bru, D.; Stres, B.; Hallet, S.; Philippot, L. Quantitative detection of the *nosZ*
542 gene, encoding nitrous oxide reductase, and comparison of the abundances of 16S
543 rRNA, *narG*, *nirK*, and *nosZ* genes in soils. *Appl. Environ. Microbiol.* **2006**, *72*, (8),
544 5181-5189.

- 545 (25) Jones, C. M.; Graf, D. R.; Bru, D.; Philippot, L.; Hallin, S. The unaccounted yet
546 abundant nitrous oxide-reducing microbial community: a potential nitrous oxide sink.
547 *ISME J.* **2013**, 7, (2), 417-426.
- 548 (26) Di, H. J.; Cameron, K. C.; Podolyan, A.; Robinson, A. Effect of soil moisture status
549 and a nitrification inhibitor, dicyandiamide, on ammonia oxidizer and denitrifier growth
550 and nitrous oxide emissions in a grassland soil. *Soil Biol. Biochem.* **2014**, 73, 59-68.
- 551 (27) Stoliker, D. L.; Repert, D. A.; Smith, R. L.; Song, B.; LeBlanc, D. R.; McCobb, T. D.;
552 Conaway, C. H.; Hyun, S. P.; Koh, D.-C.; Moon, H. S. Hydrologic controls on nitrogen
553 cycling processes and functional gene abundance in sediments of a groundwater flow-
554 through lake. *Environ. Sci. Technol.* **2016**, 50, (7), 3649-3657.
- 555 (28) Binder, B. J.; Liu, Y. C., Growth rate regulation of rRNA content of a marine
556 *Synechococcus* (Cyanobacterium) strain. *Appl. Environ. Microbiol.* **1998**, 64, (9), 3346-
557 3351.
- 558 (29) Yoon, S.; Sanford, R. A.; Löffler, F. E., *Shewanella* spp. use acetate as an electron
559 donor for denitrification but not ferric iron or fumarate reduction. *Appl. Environ.*
560 *Microbiol.* **2013**, 79, (8), 2818-2822.
- 561 (30) Park, D.; Kim, H.; Yoon, S. Nitrous oxide reduction by an obligate aerobic bacterium
562 *Gemmatimonas aurantiaca* strain T-27. *Appl. Environ. Microbiol.* **2017**, 83, (12),
563 e00502-17.
- 564 (31) Ritalahti, K. M.; Amos, B. K.; Sung, Y.; Wu, Q.; Koenigsberg, S. S.; Löffler, F. E.
565 Quantitative PCR targeting 16S rRNA and reductive dehalogenase genes
566 simultaneously monitors multiple *Dehalococcoides* strains. *Appl. Environ. Microbiol.*
567 **2006**, 72, (4), 2765-2774.
- 568 (32) Edgar, R. C. MUSCLE: multiple sequence alignment with high accuracy and high
569 throughput. *Nucleic Acids Res.* **2004**, 32, (5), 1792-1797.

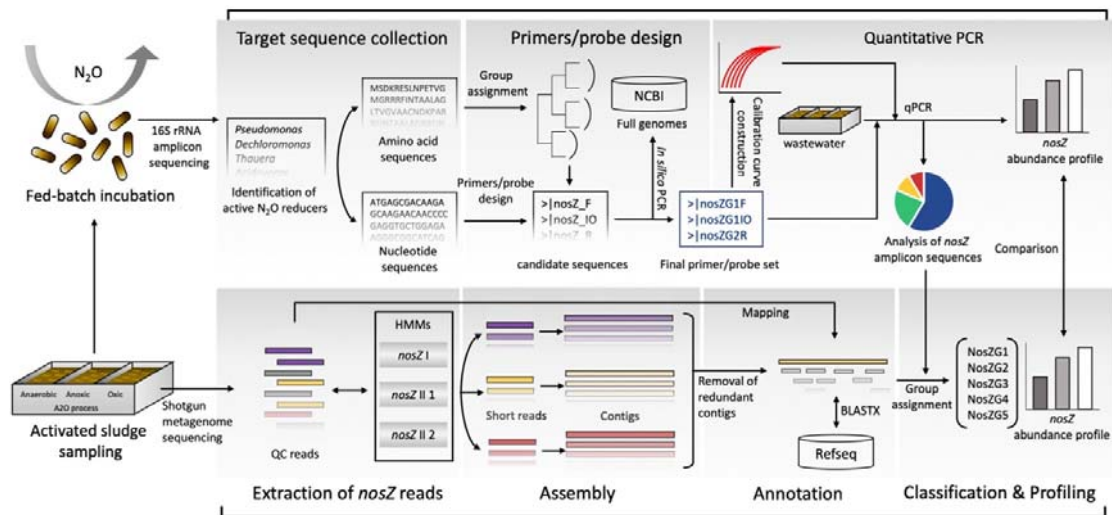
- 570 (33) Kumar, S.; Stecher, G.; Tamura, K. MEGA7: Molecular Evolutionary Genetics
571 Analysis version 7.0 for bigger datasets. *Mol. Biol. Evol.* **2016**, *33*, (7), 1870-1874.
- 572 (34) Hysom, D. A.; Naraghi-Arani, P.; Elsheikh, M.; Carrillo, A. C.; Williams, P. L.;
573 Gardner, S. N. Skip the alignment: degenerate, multiplex primer and probe design using
574 K-mer matching instead of alignments. *PloS One* **2012**, *7*, (4), e34560.
- 575 (35) Gardner, S. N.; Slezak, T. J. B. B. Simulate_PCR for amplicon prediction and
576 annotation from multiplex, degenerate primers and probes. *BMC Bioinformatics* **2014**,
577 *15*, (1), 237.
- 578 (36) Yoon, S.; Cruz-Garcia, C.; Sanford, R.; Ritalahti, K. M.; Löffler, F. E. Denitrification
579 versus respiratory ammonification: environmental controls of two competing
580 dissimilatory $\text{NO}_3^-/\text{NO}_2^-$ reduction pathways in *Shewanella loihica* strain PV-4. *ISME*
581 *J.* **2015**, *9*, (5), 1093-1104.
- 582 (37) Li, W.; Godzik, A. Cd-hit: a fast program for clustering and comparing large sets of
583 protein or nucleotide sequences. *Bioinformatics* **2006**, *22*, (13), 1658-1659.
- 584 (38) Bolger, A. M.; Lohse, M.; Usadel, B. Trimmomatic: a flexible trimmer for Illumina
585 sequence data. *Bioinformatics* **2014**, *30*, (15), 2114-2120.
- 586 (39) Nurk, S.; Meleshko, D.; Korobeynikov, A.; Pevzner, P. A. metaSPAdes: a new
587 versatile metagenomic assembler. *Genome Res.* **2017**, *27*, (5), 824-834.
- 588 (40) Li, H.; Handsaker, B.; Wysoker, A.; Fennell, T.; Ruan, J.; Homer, N.; Marth, G.;
589 Abecasis, G.; Durbin, R. The sequence alignment/map format and SAMtools.
590 *Bioinformatics* **2009**, *25*, (16), 2078-2079.
- 591 (41) Miller, C. S.; Baker, B. J.; Thomas, B. C.; Singer, S. W.; Banfield, J. F. EMIRGE:
592 reconstruction of full-length ribosomal genes from microbial community short read
593 sequencing data. *Genome Biol.* **2011**, *12*, (5), R44.

- 594 (42) Huang, Y.; Gilna, P.; Li, W. Identification of ribosomal RNA genes in metagenomic
595 fragments. *Bioinformatics* **2009**, *25*, (10), 1338-1340.
- 596 (43) Pjevac, P.; Schaubberger, C.; Poghosyan, L.; Herbold, C. W.; van Kessel, M. A. H. J.;
597 Daebeler, A.; Steinberger, M.; Jetten, M. S. M.; Lücker, S.; Wagner, M.; Daims, H.
598 *amoA*-targeted polymerase chain reaction primers for the specific detection and
599 quantification of comammox *Nitrospira* in the environment. *Front. Microbiol.* **2017**, *8*,
600 1508.
- 601 (44) Meinhardt, K. A.; Bertagnolli, A.; Pannu, M. W.; Strand, S. E.; Brown, S. L.; Stahl, D.
602 A. Evaluation of revised polymerase chain reaction primers for more inclusive
603 quantification of ammonia-oxidizing archaea and bacteria. *Environ. Microbiol. Rep.*
604 **2015**, *7*, (2), 354-363.
- 605 (45) Ma, Y.; Zilles, J. L.; Kent, A. D. An evaluation of primers for detecting denitrifiers via
606 their functional genes. *Environ Microbiol* **2019**, *21*, (4), 1196-1210.
- 607 (46) Chen, X.; Peltier, E.; Sturm, B. S. M.; Young, C. B. Nitrogen removal and nitrifying
608 and denitrifying bacteria quantification in a stormwater bioretention system. *Water Res.*
609 **2013**, *47*, (4), 1691-1700.
- 610 (47) Conthe, M.; Wittorf, L.; Kuenen, J. G.; Kleerebezem, R.; Hallin, S.; van Loosdrecht, M.
611 C. M. Growth yield and selection of *nosZ* clade II types in a continuous enrichment
612 culture of N₂O respiring bacteria. *Environ. Microbiol. Rep.* **2018**, *10*, (3), 239-244.
- 613 (48) Orellana, L. H.; Rodriguez-R, L. M.; Higgins, S.; Chee-Sanford, J. C.; Sanford, R. A.;
614 Ritalahti, K. M.; Löffler, F. E.; Konstantinidis, K. T. Detecting nitrous oxide reductase
615 (*nosZ*) genes in soil metagenomes: method development and implications for the
616 nitrogen cycle. *mBio* **2014**, *5*, (3), e01193-14.
- 617 (49) Cassman, K. G.; Dobermann, A.; Walters, D. T. Agroecosystems, nitrogen-use
618 efficiency, and nitrogen management. *Ambio* **2002**, *31*, (2), 132-140.

619 (50) Aulakh, M. S.; Khera, T. S.; Doran, J. W. Mineralization and denitrification in upland,
 620 nearly saturated and flooded subtropical soil. Effect of nitrate and ammoniacal
 621 nitrogen. *Biol. Fert. Soils* **2000**, *31*, (2), 162-167.

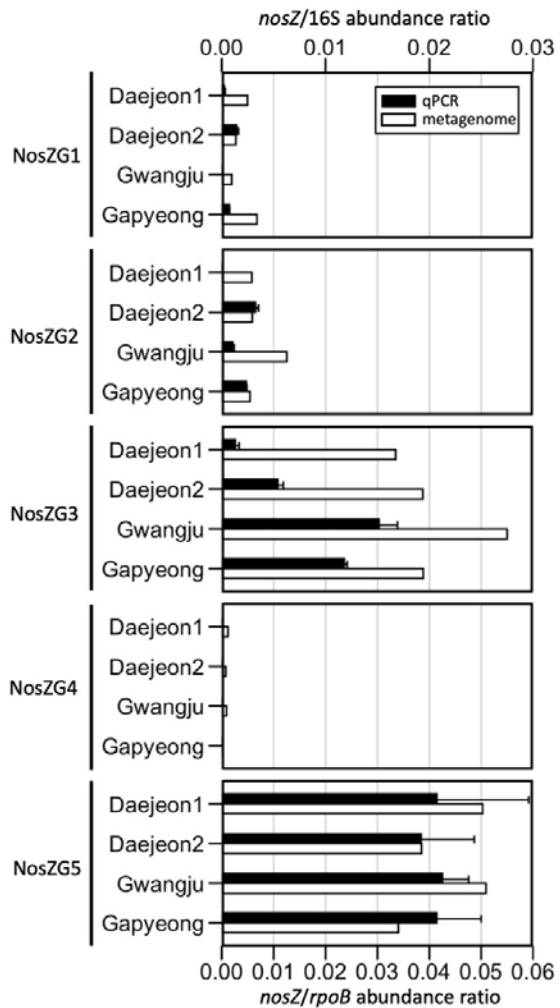
622
 623
 624
 625
 626

627 **Figures**



628

629 **Figure 1.** Flow chart for designing of the group-specific *nosZ* primer/probe sets and cross-
 630 validation with *nosZ* sequence data extracted from shotgun metagenome data

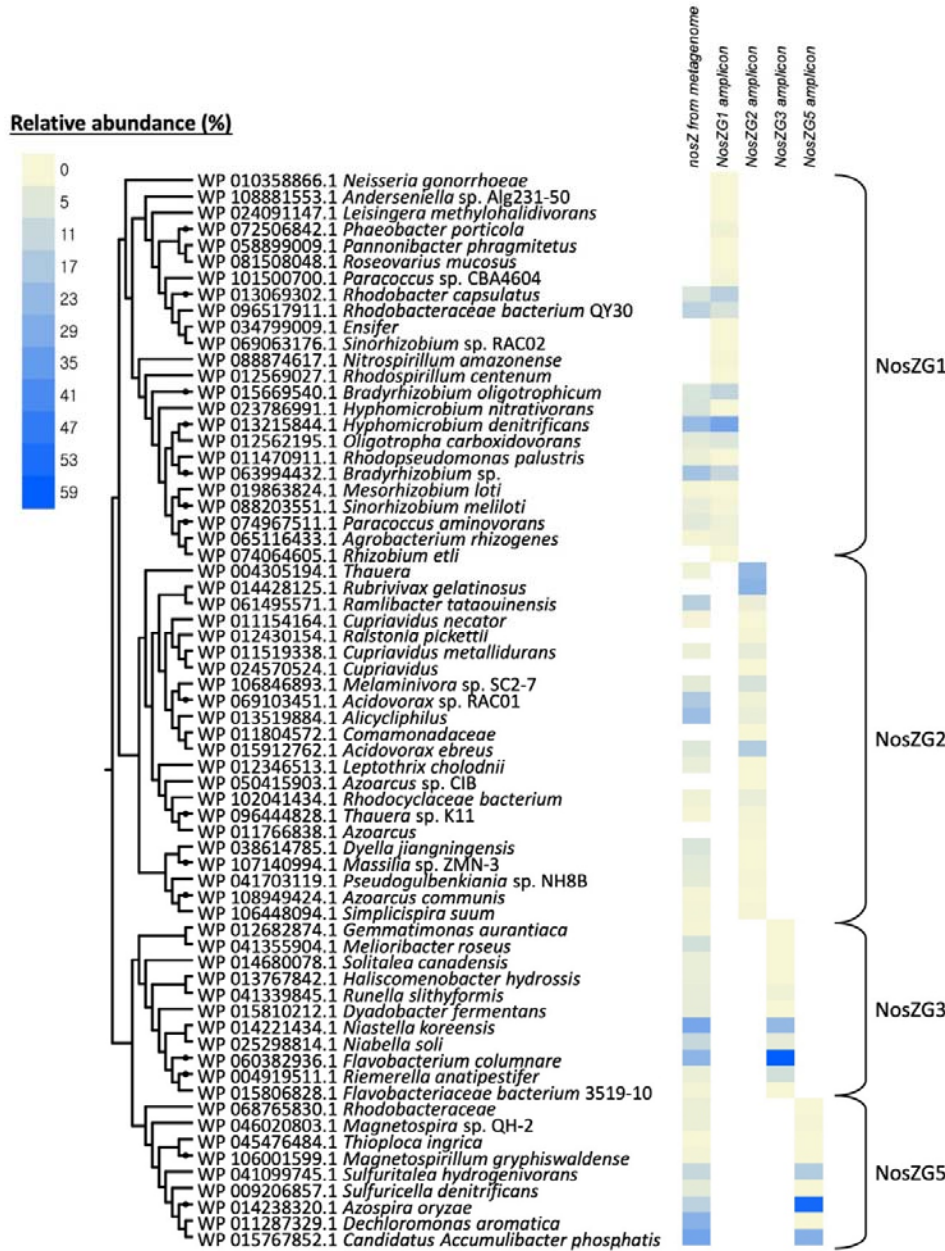


631

632 **Figure 2.** The relative abundances of NosZG1-5 *nosZ* genes as quantified using qPCR and
633 metagenome analysis. The *nosZ* copy numbers from the qPCR assays were normalized with
634 the copy numbers of eubacterial 16S rRNA genes. The coverages of *nosZ* genes in the
635 metagenome data were normalized with the coverages of *rpoB* genes. The presented qPCR
636 quantification data are the averages of triplicate samples processed separately through
637 extraction and qPCR procedures, with the error bars representing their standard deviations.

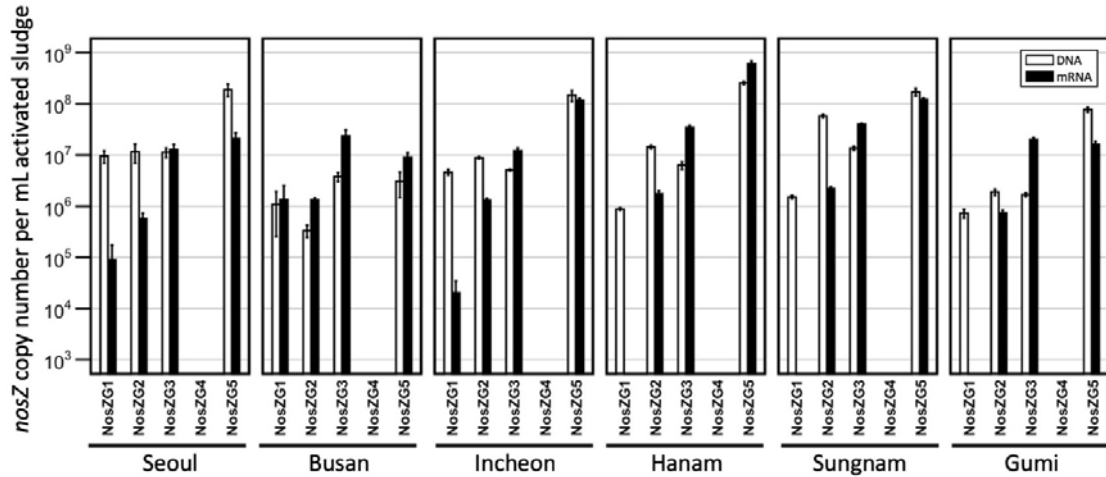
638

639



640

641 **Figure 3.** The phylogenetic tree constructed with the reference *nosZ* sequences of the taxa
 642 matching OTUs generated from the partial *nosZ* sequences amplified with NosZG1-5 primers.
 643 The phylogenetic tree was generated using neighbor-joining method with 500 bootstrap
 644 replications. The heatmap shows the relative abundances of the OTUs within each *nosZ*
 645 group, computed from the amplicon sequencing data and the *nosZ* sequence data extracted
 646 from the metagenome



647

648 **Figure 4.** The copy numbers of NosZG1-5 *nosZ* genes and transcripts in activated sludge
649 samples collected from anoxic tanks of six activated sludge-type WWTPs in Korea, as
650 quantified using the group-specific *nosZ* qPCR developed in this study. The presented data
651 are the averages of triplicate samples processed separately through extraction, purification
652 and reverse transcription (for analyses of transcripts), and qPCR procedures, with the error
653 bars representing their standard deviations.

654

655

656

657

658

659

660

661

662

663

664

665

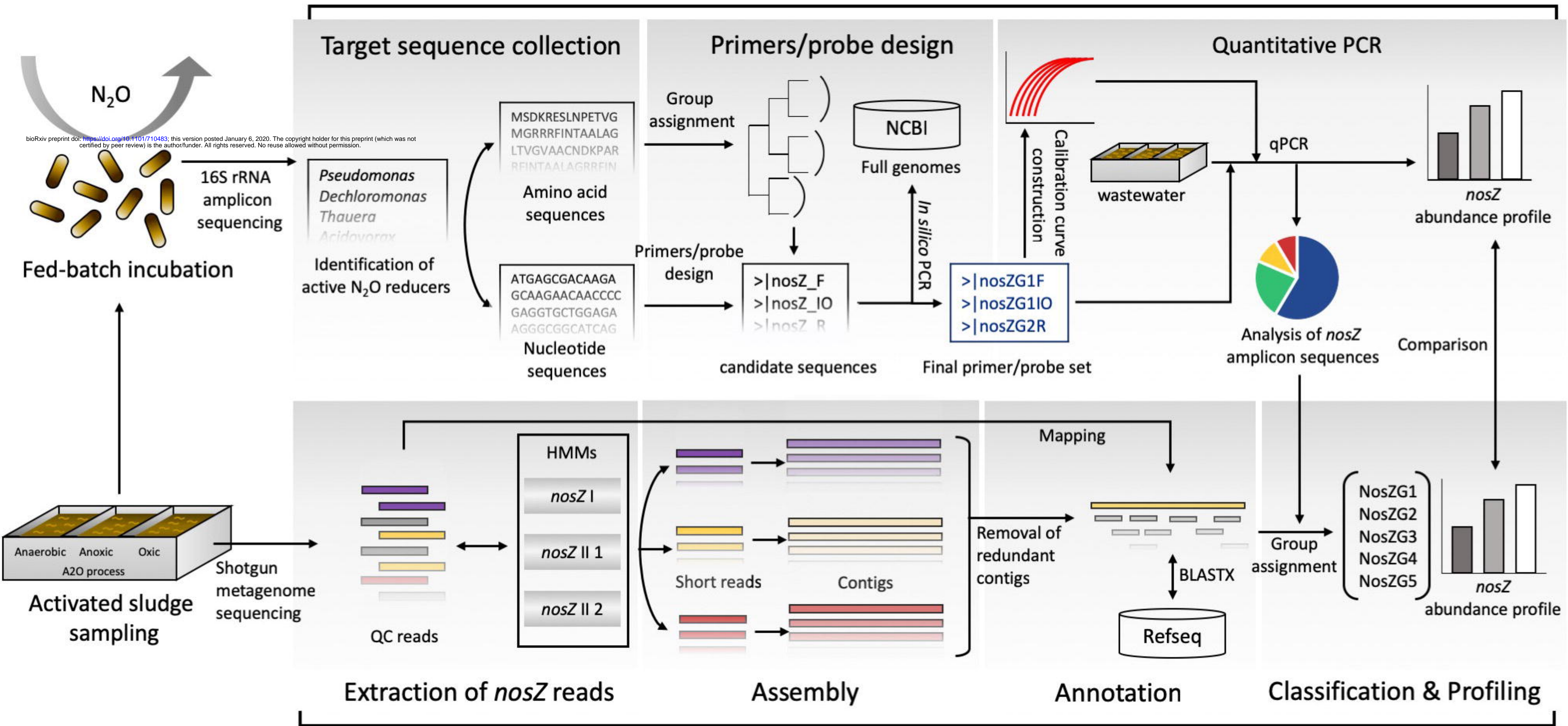
666 Table 1. The primers/probe sets developed in this study for group-specific quantification of
 667 *nosZ* genes

668

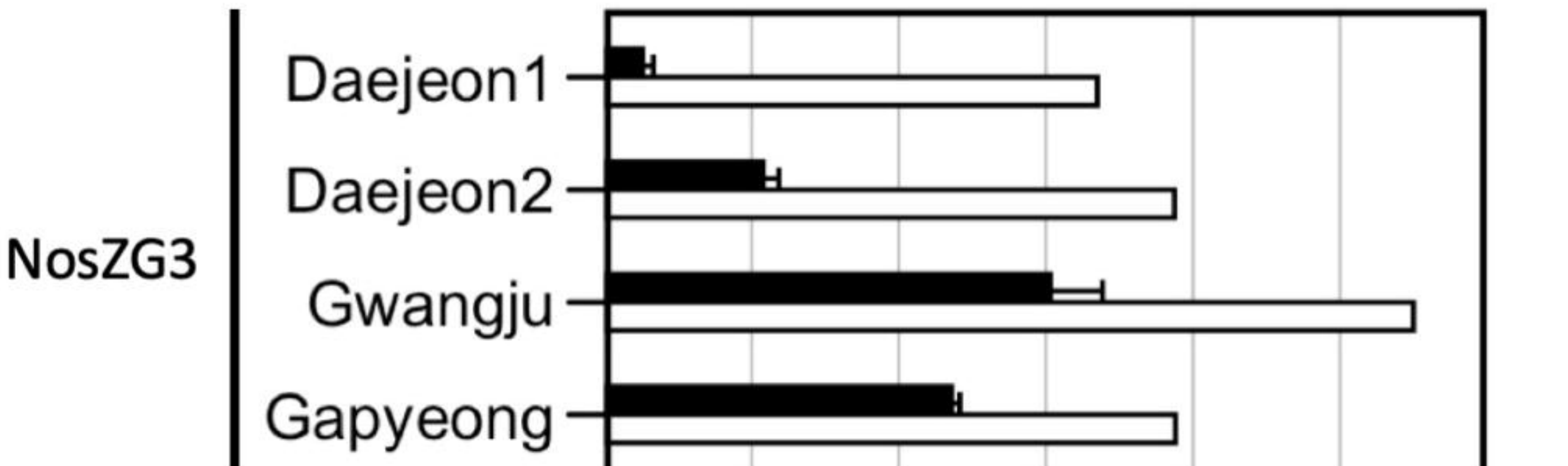
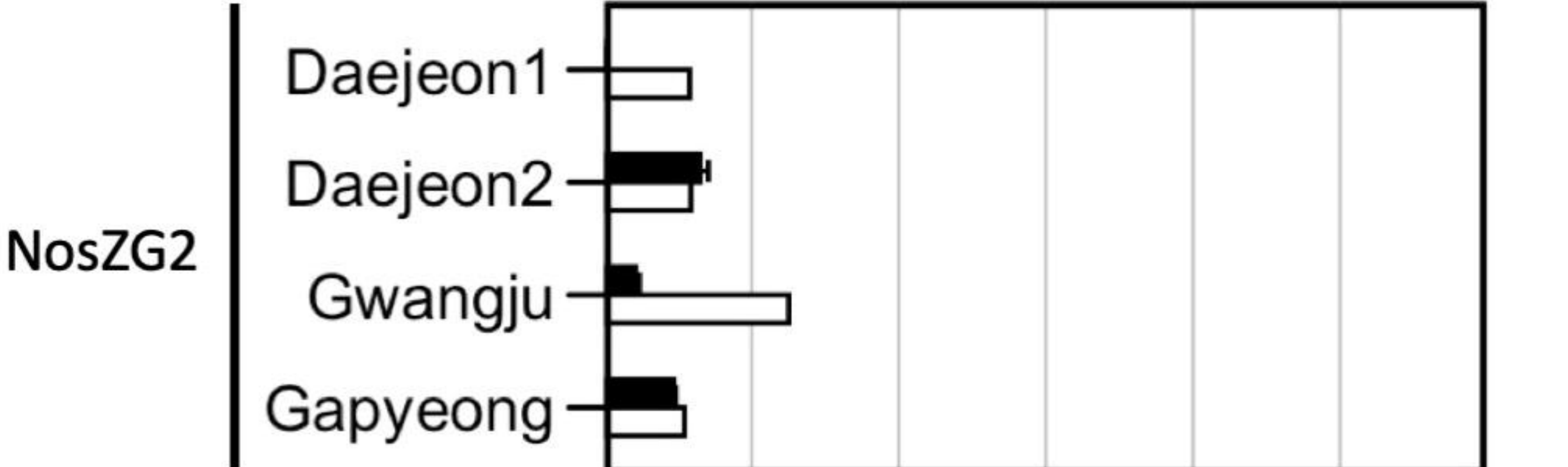
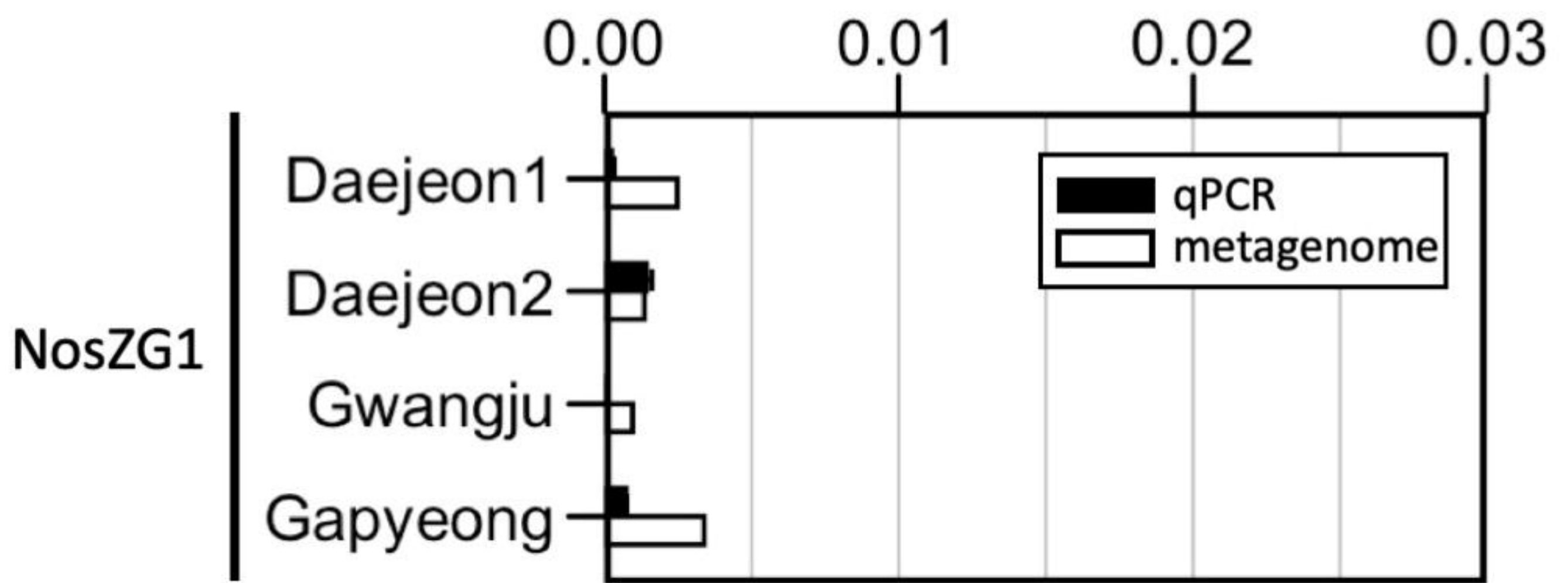
Targeted group	Primers / Probe	Sequence (5' → 3')	Degeneracy	Coverage	Efficiency (%)
NosZG1	NosZG1F	AAG GTN CGB GTN TAC ATG	48	70% (77/110)	91.6
	NosZG1R	CSN NCA TYT CCA TGT GCA	64		
	NosZG1P	FAM-ACT GCM VBT GGT TCT GCC AYG C-MGBNFQ	36		
NosZG2	NosZG2F	GRC ATC WKC MMC GAC AAG	32	84.4% (27/32)	93.4
	NosZG2R	HYC TCG RYG TTG TAC TGG	24		
	NosZG2P	FAM-ACC ACS CGC GTG TTC TGC G-MGBNFQ	2		
NosZG3	NosZG3F	CAY TTT GCW CCD GAY AAT ATT GAA	24	95% (19/22)	90.7
	NosZG3R	BSH WGT TTC ACC BGG CAT	108		
	NosZG3P	FAM-AA YTR GAA CAA GAY TGG GAT GTA CCK C-MGBNFQ	32		
NosZG4	NosZG4F	ATW GTT GCY GGH GGM AAA	24	57.1% (4/7)	94.9
	NosZG4R	TTC CCA DGT KCC DAW TTT	36		
	NosZG4P	FAM-MGG YGA AGT KSA GAA TCC GGG WT-MGBNFQ	32		
NosZG5	NosZG5F	AAC GAC AAG KCS AAY CCG	8	100% (5/5)	97.7
	NosZG5R	GCG GTC GAA CTT CCA GTA	0		
	NosZG5P	FAM-GCS GTG MTC GAY CTG CGB G-MGBNFQ	24		

670

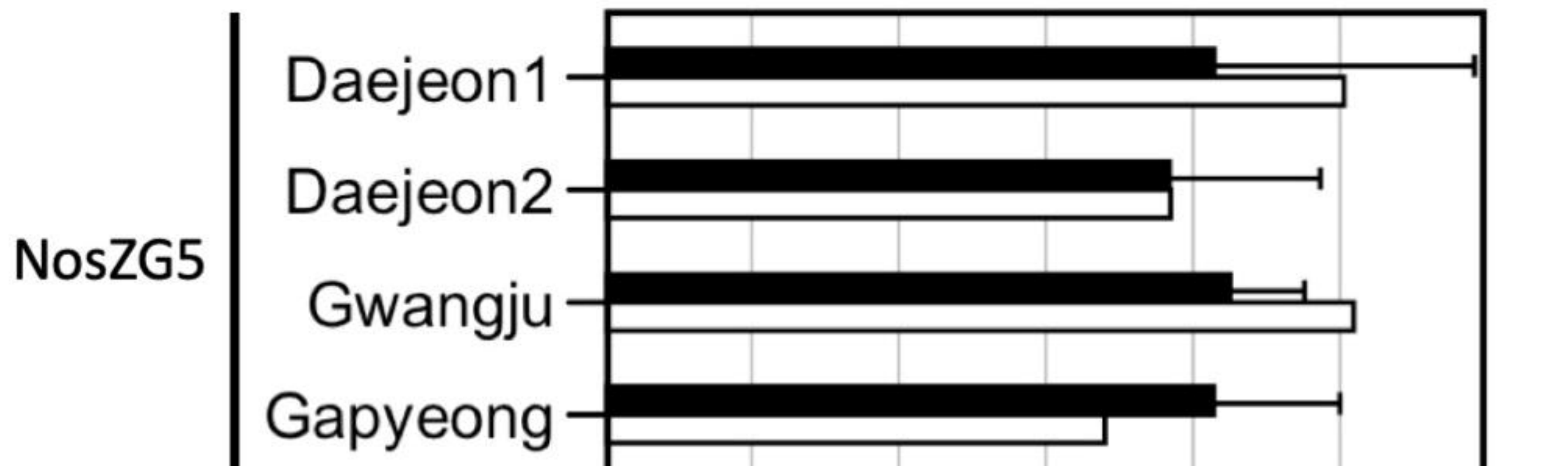
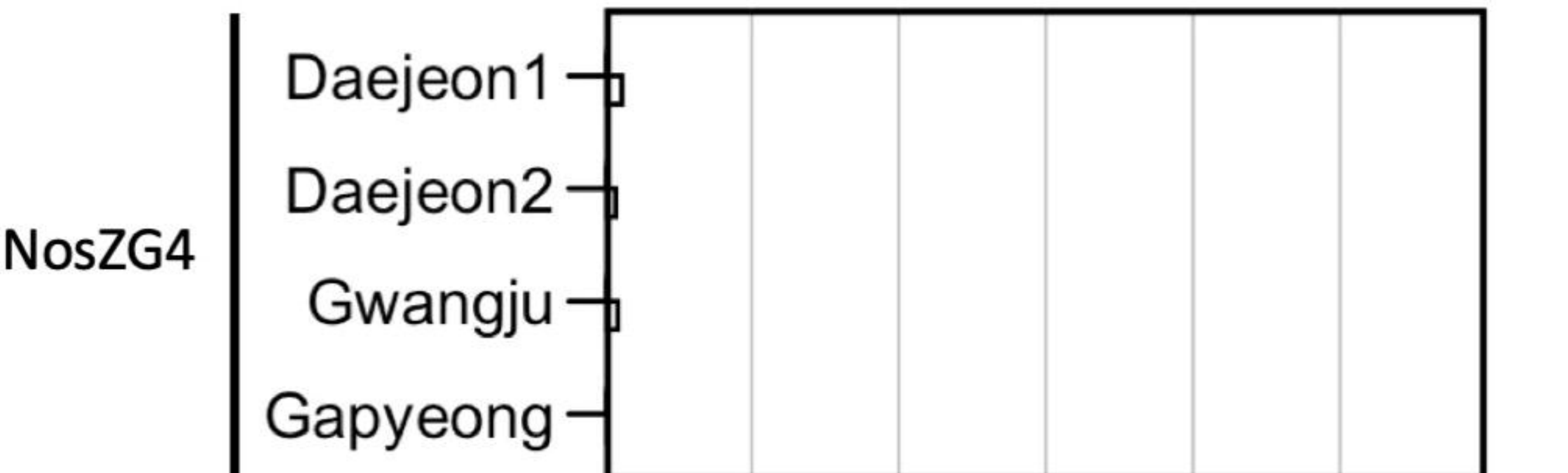
bioRxiv preprint doi: <https://doi.org/10.1101/710483>; this version posted January 6, 2020. The copyright holder for this preprint (which was not certified by peer review) is the author/funder. All rights reserved. No reuse allowed without permission.



nosZ/16S abundance ratio

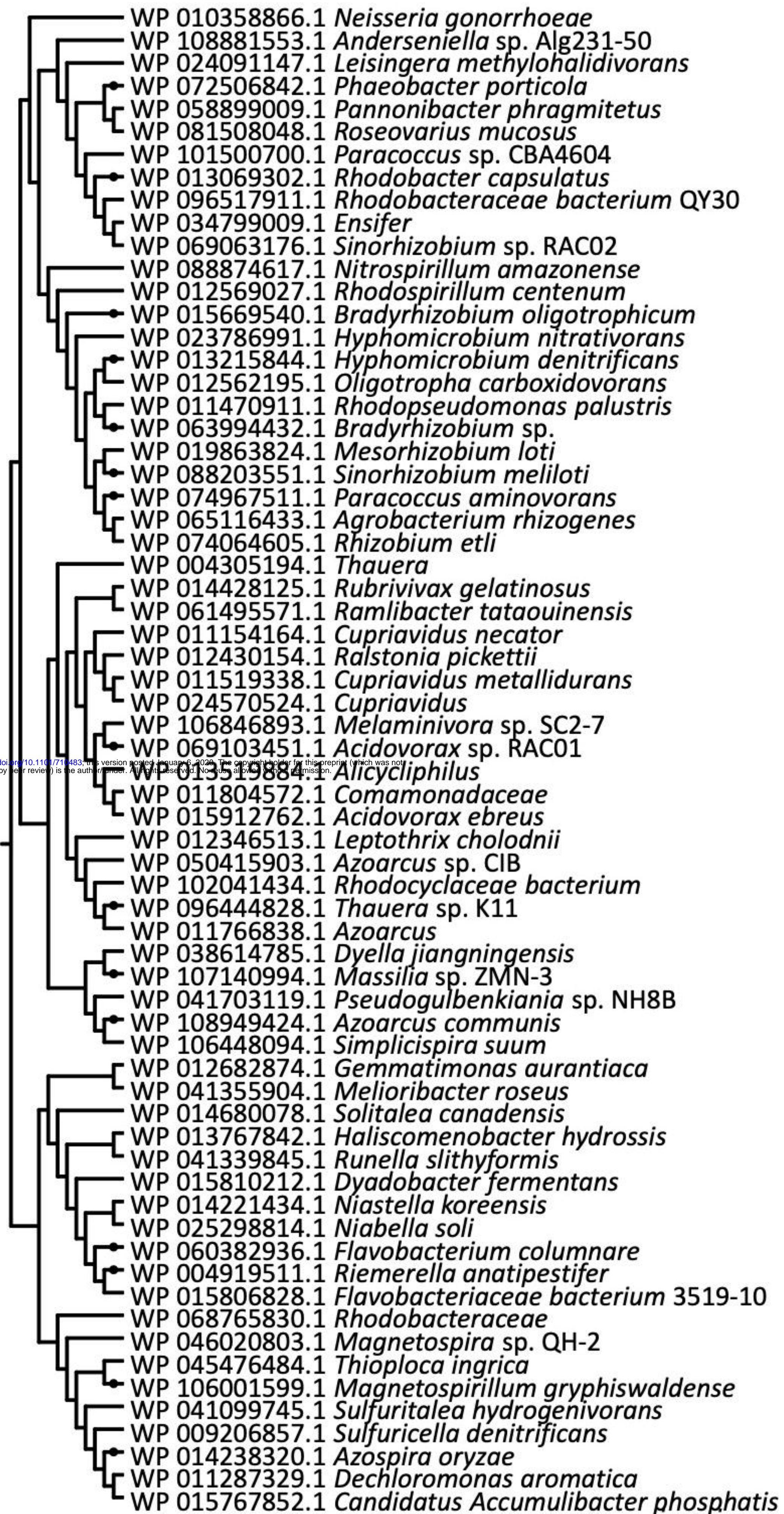
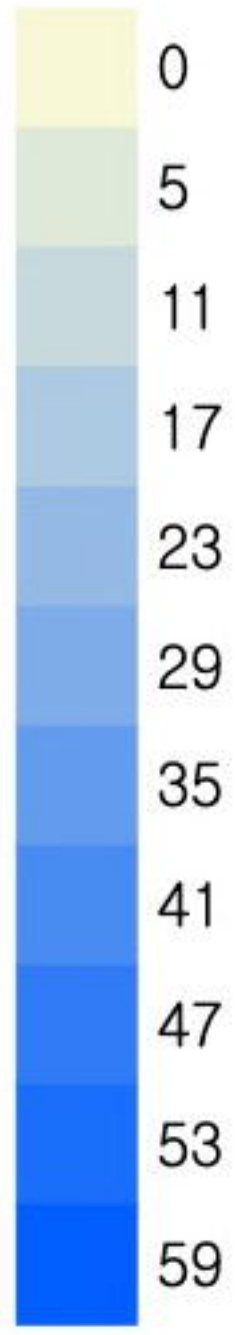


bioRxiv preprint doi: <https://doi.org/10.1101/710483>; this version posted January 6, 2020. The copyright holder for this preprint (which was not certified by peer review) is the author/funder. All rights reserved. No reuse allowed without permission.



nosZ/*rpoB* abundance ratio

Relative abundance (%)



nosZ from metagenome
 NosZG1 amplicon
 NosZG2 amplicon
 NosZG3 amplicon
 NosZG5 amplicon



NosZG1

NosZG2

NosZG3

NosZG5

bioRxiv preprint doi: <https://doi.org/10.1101/711483>; this version posted August 6, 2020. The copyright holder for this preprint (which was not certified by peer review) is the author/funder. All rights reserved. No reuse allowed without permission.

nosZ copy number per mL activated sludge

